J. Am. Soc. Mass Spectrom. (2019) 30:1631–1642
DOI: 10.1007/s13361-019-02227-1

RESEARCH ARTICLE

ETD-Cleavable Linker for Confident Cross-linked Peptide Identifications

Bingqing Zhao, Colin P. Reilly, James P. Reilly

Department of Chemistry, Indiana University, 800 East Kirkwood Avenue, Bloomington, IN 47405, USA

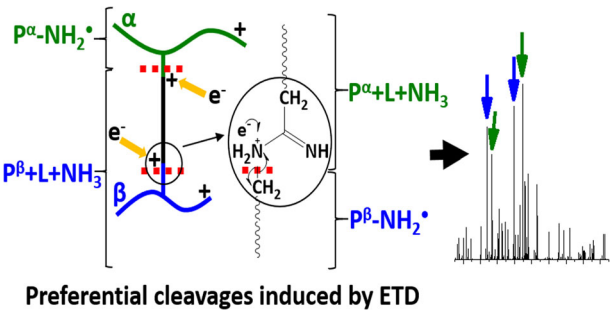

Preferential cleavages induced by ETD

Abstract. Peptide cross-links formed using the homobifunctional-linker diethyl suberthioimidate (DEST) are shown to be ETD-cleavable. DEST has a spacer arm consisting of a 6-carbon alkyl chain and it cleaves at the amidino groups created upon reaction with primary amines. In ETD MS^2 spectra, DEST cross-links can be recognized based on mass pairs consisting of peptide-$NH_2^{\bullet}$ and peptide+linker+NH_3 ions, and backbone cleavages are more equally distributed over the two constituent peptides compared with collisional activation. Dead ends that are often challenging to distinguish from cross-links are diagnosed by intense reporter ions. ETD mass pairs can be used in MS^3 experiments to confirm cross-link identifications. These features provide a simple but reliable approach to identify cross-links that should facilitate studies of protein complexes.

Keywords: Cross-linking, Electron transfer dissociation

Received: 18 December 2018/Revised: 12 April 2019/Accepted: 13 April 2019/Published Online: 16 May 2019

Introduction

Chemical cross-linking combined with mass spectrometry is commonly utilized to study topological features and interactions of proteins by establishing structural distance constraints [1–5]. This rapidly emerging technique has unveiled structures and interactions of protein complexes [6–12] and networks [13, 14]. Nonetheless, interpretation of MS/MS spectra of cross-links is universally recognized as challenging due to the quadratically augmented computational search space and the unequal fragmentation efficiency of the two linked peptides [14, 15]. Confusion of isobaric cross-link and dead-end species, incomplete fragmentation of cross-linked products as well as low mass accuracy fragment ion data also lead to ambiguous matches, and it has been argued that reported cross-links are often incorrect [16]. Approaches that provide more definitive identifications of cross-links are needed.

Cleavable cross-linkers were introduced to reduce some of the above problems through the formation of diagnostic fragmentation patterns, such as reporter ions and peak doublets associated with constituent peptides [17]. A number of cross-linkers cleavable by collision-induced dissociation (CID) have been introduced, such as protein interaction reporters (PIR) [18, 19], disuccinimidyl-succinamyl-aspartyl-proline (SuDP) with its derivatives [20–22], BuUrBu (DSBU) [23] with its derivatives [24], disuccinimidyl sulfoxide (DSSO) [25] with its derivatives [26, 27], DC4 [28], and cyanurbiotindipropionylsuccinimide (CBDPS) [29]. All of these incorporate functional groups that form labile sites along the spacer arms of cross-linkers. In a common workflow with cleavable linkers, characteristic cross-link fragments are observed in MS^2 spectra. In some cases, such as with BuUrBu, sequences of the cross-linked peptides are identified from backbone fragments in MS^2 spectra [30]. In others, such as with DSSO, intact peptide peaks from MS^2 spectra are further fragmented [25].

Cross-linkers cleavable by electron transfer dissociation (ETD) have received considerably less attention. ETD is an activation method that leaves many CID labile sites intact and is relatively indifferent to the sequences of peptides [31]. These features make ETD widely implemented in top-down

Electronic supplementary material The online version of this article (https://doi.org/10.1007/s13361-019-02227-1) contains supplementary material, which is available to authorized users.

Correspondence to: James Reilly; *e-mail:* reilly@indiana.edu

proteomics [32–34] and in characterizing post-translational modifications (PTMs) [34–36]. Interestingly, ETD sometimes outperforms CID and higher energy collisional dissociation (HCD) for peptide identification of highly charged or low *m/z* precursors [37, 38]. A recent study with disuccinimidyl suberate (DSS) and bis(sulfosuccinimidyl)suberate (BS3) cross-links showed encouraging results: ETD with supplementary activation of HCD (EThcD) led to the best sequence coverage for highly charged cross-links [39]. Cross-linkers with ETD-cleavable features might enhance the confidence of cross-link identifications. However, only a few ETD-cleavable cross-linkers have been reported. Bis-arylhydrazone (BAH) cross-linked peptides cleave at the N-N hydrazone bond yielding one radical peptide and one even-electron peptide. MS^3 experiments on these two peaks generate nearly complete sequence coverage [40]. Based on this, an ETD and CID dual cleavable cross-linker, DUCCT, was introduced and has been applied to standard peptides and proteins [41]. Another ETD-cleavable cross-linker, 1,3-diformyl-5-ethynylbenzene (DEB), forms cross-links through reductive amination. DEB cross-linked peptides maintain the two protonation sites of amino moieties and yield diagnostic ions that reveal the intact unmodified constituent peptides [42]. These encouraging developments suggest that ETD-cleavable cross-linkers with different sizes, polarities, reactive chemistries, and cleavage propensities may find useful applications.

While carboxyl-reactive cross-linkers [43, 44] and heterobifunctional cross-linkers [45] have been reported, most cross-linkers react with primary amines of lysine residues and protein N-termini. With few exceptions [42, 46, 47], nearly all reported amine-reactive cleavable cross-linkers that have demonstrated efficacy with proteins at physiological conditions (pH ≈ 7.4) utilize *N*-hydroxysuccinimide (NHS) ester reactive groups. A disadvantage they share is that these cross-linkers acylate primary amines, and therefore neutralize their positive charge. This may result in disruptions of the electrostatic properties of proteins and reduction of the charge states of cross-linked peptides. The latter would not facilitate their ETD fragmentation.

Previously, we developed diethyl suberthioimidate (DEST) [48], a cross-linker that reacts with primary amines to form amidino linkages that are highly basic and preserve the charge on amines at physiological pH. DEST has a simple six-carbon spacer arm and thioimidate groups at both ends. The structures of DEST and its cross-linking product as well as the most abundant hydrolyzed dead end [48, 49] are depicted in Scheme 1. Its structure is derived from *S*-methyl thioacetimidate (SMTA), a peptide and protein labeling reagent comprising one thioimidate reactive group [50–54]. Since proteins labeled by SMTA maintain their functions [55] and native structures [56–58], DEST cross-linking is unlikely to perturb structure. Also, the two positive charges retained on the amidino linkages should enable more effective enrichment of DEST cross-links with strong cation exchange chromatography (SCX) [12] compared to cross-links of NHS-ester cross-linkers that lack these positive charges. With DEST, we have probed the native structure of model protein cytochrome c [48], the *E. coli* ribosome [12], and established the location of *E. coli* ribosomal protein S1 [11]. Meanwhile, another amidinating cross-linker, dimethyl suberimidate (DMS), also reacts with primary amines to form the same amidine groups. However, as an imidoester rather than a thioimidoester, DMS requires a strongly alkaline environment (pH > 9) to maximize its cross-linking efficiency [59]. It forms almost no cross-links at physiological pH [60] compromising studies of native protein structures. Nevertheless, when the reaction is done at high pH, DMS reportedly produces more highly charged cross-links than the acylating reagent DSS [61]. In addition to their improved SCX enrichment efficiency, the highly charged DEST cross-links are attractive candidates for fragmentation using ETD.

In this work, we investigated the ETD fragmentation patterns of DEST cross-linked peptides and dead-end peptides. Exploiting their unique diagnostic features, we developed an ETD MS^2-based approach to facilitate identifications of DEST cross-links and enable on-the-fly differentiation between cross-links and dead ends. HCD MS^3 experiments on individual peptides from cross-links were automatically implemented to validate identifications from ETD MS^2 spectra. This approach was demonstrated in model studies of cytochrome c and ubiquitin. These simple systems were selected to observe cross-link fragmentation propensities because the identities of cross-links are virtually unambiguous. The simplicity of the sample also results in spectra with particularly good signal-to-noise ratios. Because the fragmentation of cross-linked peptides is independent of the complexity of their source, cross-links derived from other biological systems yield spectra that display similar ion types and fragmentation patterns.

Experimental

Chemicals and Reagents

Equine cytochrome c, bovine ubiquitin, proteomics grade trypsin, Tris hydrochloride, Tris base, suberonitrile, and ethanethiol were purchased from Sigma-Aldrich (St. Louis, MO). Anhydrous diethyl ether, Optima® grade water, and Optima® grade acetonitrile (ACN) were ordered from Fisher Scientific (Hampton, NH). Dichloromethane and sulfuric acid were procured from EMD Millipore (Burlington, MA). Sodium chloride and ammonium bicarbonate were supplied by Avantor Performance Materials (Center Valley, PA). Formic acid (FA) was provided by Acros Organics (Waltham, MA).

Protein Cross-linking Experiments

DEST was synthesized in-house as previously described and discussed in Supporting Information [48]. Five micromolar equine cytochrome c and 10 μM bovine ubiquitin were reacted with DEST at molar ratios of 1:100 and 1:50 respectively in 50 mM Tris buffer (pH 7.4). After 4 h, the reactions were quenched with 100 mM ammonium bicarbonate buffer

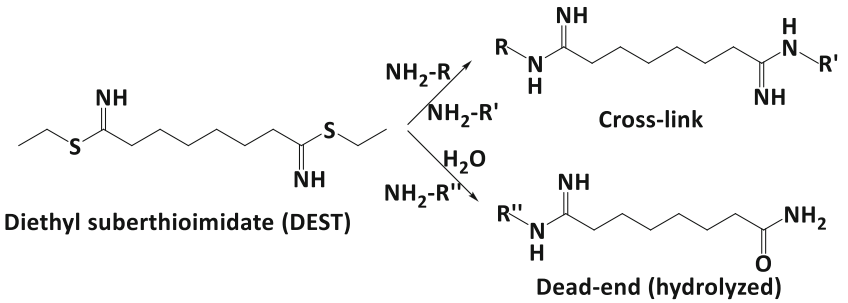

Scheme 1. DEST and its major reaction products

(pH 7.8). Centrifugal filters with 3 kDa molecular weight cutoff (Millipore, Burlington, MA) were used to clear hydrolyzed DEST and exchange the products to 50 mM ammonium bicarbonate buffer (pH 7.8).

Digestion of Cross-linked Proteins

Proteomics grade trypsin was added to DEST cross-linked protein solutions at a 1:20 (*w*/*w*) ratio of protease to substrates in 50 mM ammonium bicarbonate buffer. Samples were incubated for 18 h at 37 °C with constant rotation after which FA was added to a concentration of 1%. Digests were dried in a SpeedVac and stored at – 20 °C.

Nano-HPLC/Nano-ESI MS^2 or MS^3 Analysis

Tryptic digests were analyzed with an Orbitrap Fusion Lumos Tribrid mass spectrometer (Thermo Fisher Scientific, Waltham, MA) coupled with an EASY-nLC 1200 liquid chromatograph (Thermo Fisher Scientific, Waltham, MA). Between 0.1 and 0.5 µg of tryptic digest was loaded onto a C18 trap column with mobile phase A (0.1% FA in water), and then separated by an Acclaim PepMap RSLC C18 column (75 µm× 25 cm, 2 µm, 100 Å) (Thermo Fisher Scientific, Waltham, MA) with a 30-min or 60-min gradient from 2 to 50% mobile phase B (0.1% FA, 80% ACN, and 19.9% water) at 300 nL/min. Eluting species were ionized by nano-electrospray with a spray voltage of 1900 V. Full scan spectra were recorded at a resolution of 120 K.

For MS^2 analysis, the data-dependent mode was utilized to fragment the most abundant peaks by CID with a 35% normalized collision energy or ETD with 40 or 50 ms reaction time. The cycle time was set at 5 s. Precursor ions in charge states of 3+ to 7+ were subjected to fragmentation with an isolation window of 2.0 *m/z*, a maximum ion injection time of 100 ms and AGC of 5E5. All MS^2 spectra were recorded in an orbitrap in one microscan with a resolution of 30 K.

ETD fragment ions with a mass spacing of 169.1453 Da were further selected in data-dependent mode and activated by HCD in an ion-routing multipole (HCD cell) with 35% collision energy. The precursor isolation window was set at 2.5 *m/z*. A maximum ion injection time of 200 ms and AGC of 5E5 were applied. Product masses were analyzed in a linear ion trap with one microscan.

Data Analysis

Raw data files were converted to *.mgf files by Proteome Discoverer 2.1 software (Thermo Fisher Scientific, Waltham, MA). Precursors, charge reduced precursors and neutral loss fragments within 18.5 Da of the precursors were removed from all ETD MS^2 mass lists. All spectra were interpreted with an in-house program that computes metrics such as precursor mass errors, numbers of peaks matched for each constituent peptide, percentages of ion intensities matched to each constituent peptide, and scores for tentative identifications. ETD and CID MS^2 spectra were interpreted as arising from cross-links, dead ends, loop links, and regular peptides against a target database of equine cytochrome c or bovine ubiquitin concatenated with two different decoy databases: one containing ten randomized versions of the target protein sequence and a second one containing 55 *E. coli* ribosomal proteins. All MS^2 spectra were searched with precursor mass tolerance of 5 ppm and fragment mass tolerance of 10 ppm. Up to three missed cleavages were considered, and oxidation of methionine was allowed as a variable modification. MS^3 spectra of ETD product ions were matched to tentative sequences that had been derived from MS^2 spectra. All MS^3 spectra were searched with a mass tolerance of 0.2 Da, which is compliant with the lower mass accuracy of ion traps. All cross-link identifications were manually checked to verify that more than 50% of the total fragment ion intensity was assigned. For cross-links matched from ETD spectra, a minimum of two mass pair peaks was required. For cross-links found in CID spectra, the percentage of peaks matched to tentative identification was required to exceed 35%, and a minimum of two peaks was required to match fragments derived from each constituent peptide. The above criteria led to FDR < 1% with both ETD and CID approaches. All cross-links satisfying these criteria are tabulated in Tables S1 and S2 of Supporting Information. Most of the data are significantly better than the minimal criteria just mentioned. For example, on average, 82.7% of ETD fragment ion intensities were assignable and 83.6% (123 out of 147) of the spectra contained all four mass pair peaks. Likewise, 83.8% of the CID fragment ion intensities were assignable. In plotted mass spectra, the most intense peak in each isotope cluster is displayed. The precursor ions presented in the spectra were not considered in calculated numbers of matched peaks, percentages of fragment ion intensities matched, and scores.

Results and Discussion

Electron Transfer Dissociation of DEST Cross-linked Peptides

Cytochrome c and ubiquitin were each cross-linked with DEST. Following tryptic digestion, the resulting products were analyzed. For example, a quadruply charged 394.7404 *m/z* ion from cytochrome c digest was fragmented by ETD and yielded the spectrum shown in Figure 1a. Green peaks result from fragmentation of the longer peptide, that is referred to as peptide *α*; blue peaks are fragments of peptide *β*. Precursors, charge reduced precursors, and those with neutral losses of ammonia or water, are in red. Unassignable peaks are in black. This cross-link was identified as MIFAGIKK—KYIPGTK. The identity of the former peptide is established from consecutive $z^{\bullet}_1$ to $z^{\bullet}_7$, $z+1_2$ to $z+1_6$, and c_2 to c_7 ions as well as y_1 and $a+1_7$ ions. The latter is identified from $z^{\bullet}_1$ to $z^{\bullet}_3$, $z^{\bullet}_5$, $z^{\bullet}_6$, c_2, and c_4 to c_6 ions in addition to y_1, y_4, $a+1_5$, and $a+1_6$ ions. In addition to these backbone fragment ions, four intense peaks in the spectrum can be assigned to $P^{\alpha}\text{-}NH_2^{1+}$, $P^{\alpha}+L+NH_3^{2+}$, $P^{\beta}\text{-}NH_2^{1+}$, and $P^{\beta}+L+NH_3^{2+}$, where P^{α} and P^{β} refer to the two intact peptides and L represents the DEST linker. As depicted in Scheme 2, these ions are formed through cleavage of the bond between the amidino group and the adjacent carbon. Their large intensities indicate that ETD favors this cleavage site, consistent with previous observations that amidine groups are readily protonated during ESI [50, 62]. It appears that the protonated amidino groups preferentially attract electrons and are neutralized to form hypervalent species. This induces the homolytic cleavage of the adjacent N-C bonds to form $P\text{-}NH_2^{\bullet}$, a radical ion of one peptide, and $P+L+NH_3$, an even-electron species of the other peptide. Two factors favor this dissociation over the formation of conventional c- and $z^{\bullet}$-ions. First, since the amidino groups are protonated, the migration of a hydrogen atom ($H^{\bullet}$) is not necessary to initiate this N-

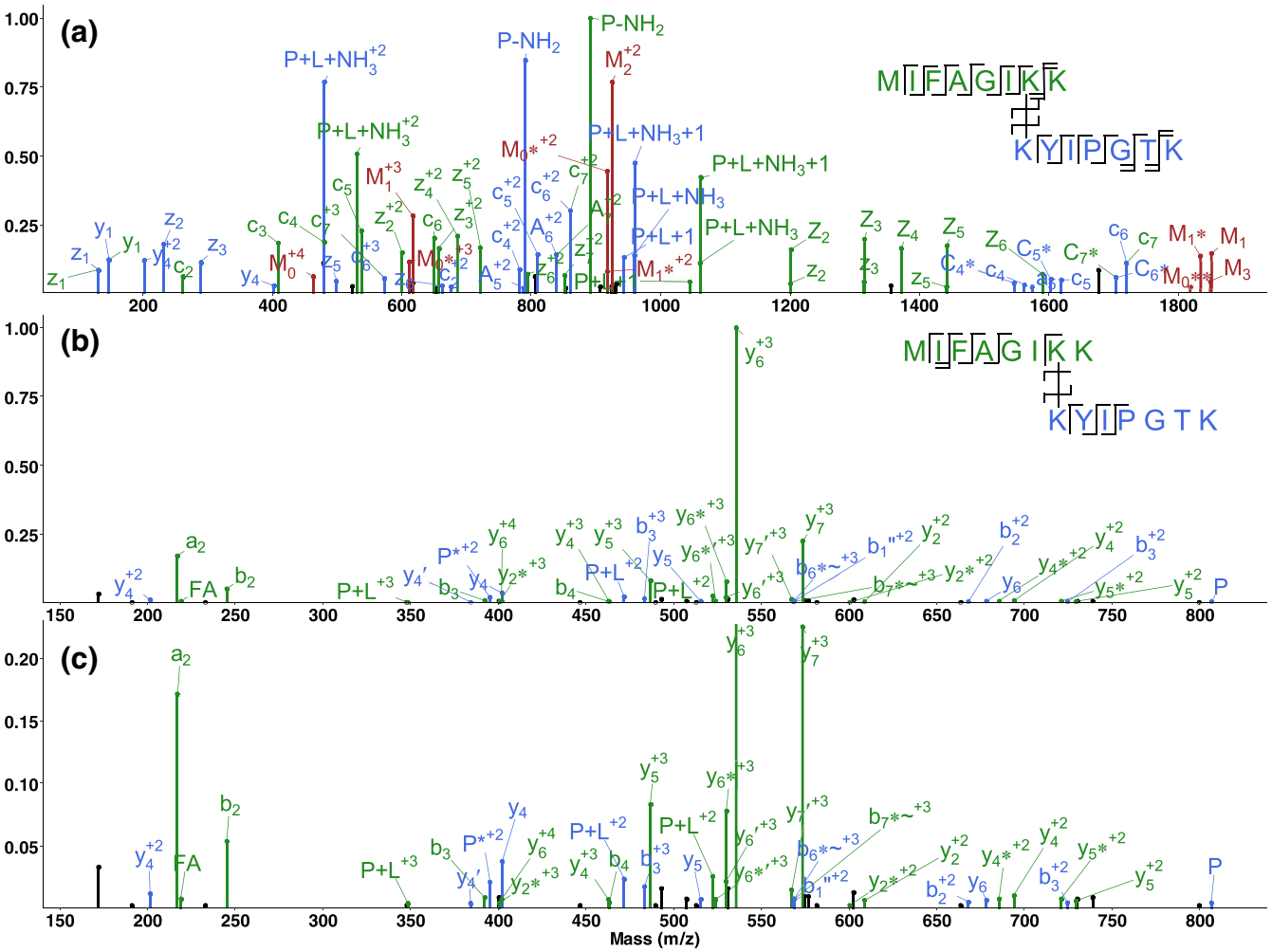

Figure 1. MS^2 spectra of the cytochrome c cross-link MIFAGIKK—KYIPGTK^{4+} fragmented by **(a)** ETD and **(b)** CID. To display the relative intensities of smaller peaks, the CID spectrum is also plotted with the y_6^{3+} ion off scale in **(c)**. Green peaks are fragments of peptide α; blue peaks are fragments of peptide β. Precursors, charge reduced precursors, and those with neutral losses of ammonia (asterisk) or water (prime) are in red. Unassignable peaks are in black. a + 1, c + 1, and z + 1 ions are represented as A, C, and Z (capitalized) ions; a tilde denotes addition of water. Subscripts following M represent the numbers of hydrogen atoms abstracted from the precursor ion after electron capture

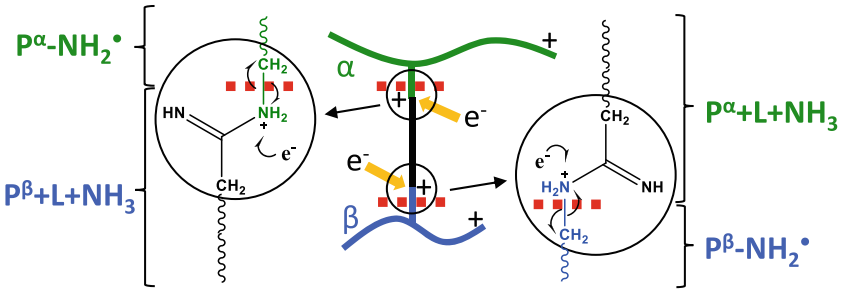

Scheme 2. Preferential cleavages induced by ETD. Structures in green belong to peptide *α*, and those in blue are associated with peptide *β*. DEST is in black

C bond dissociation, whereas it would be required to produce backbone c- and $z^{\bullet}$-ions [63, 64]. Second, the even-electron product ion $P + L + NH_3$ has stable amidine resonance structures that backbone c ions lack.

In the above example, it is likely that the two amidine groups sequester two protons, and each peptide retains one. When the proton on the amidine group associated with peptide *α* is neutralized, it forms the singly charged P^{α}-$NH_2^{\bullet}$ and the doubly charged $P^{\beta} + L + NH_3$. Likewise, when the proton on the amidine group associated with peptide *β* is neutralized, it produces singly charged P^{β}-$NH_2^{\bullet}$ and doubly charged $P^{\alpha} + L + NH_3$. In their singly charged states, P^{α}-$NH_2^{\bullet}$ and $P^{\alpha} + L + NH_3$ differ in composition by $C_8N_4H_{17}$, which corresponds to 169.1453 Da. P^{β}-$NH_2^{\bullet}$ and $P^{\beta} + L + NH_3$ have the same mass spacing. Components of mass pairs in other charge states, such as singly charged $P^{\alpha} + L + NH_3$ and $P^{\beta} + L + NH_3$ also appear in Figure 1a. These could arise either from peptides of cross-links protonated in other ways or from some charge reduction process [31]. Additionally, other mass pair-related fragments such as $P^{\alpha} + L + NH_3 + 1^{1+\bullet}$ and $P^{\beta} + L + NH_3 + 1^{1+\bullet}$ also appear. These apparently result from $P + L + NH_3^{2+}$ ions capturing an electron or $P + L + NH_3^{1+}$ ions picking up a hydrogen atom. Both processes are common in ETD [65]. The occurrence of mass pairs enhances the confidence of peptide mass determination and overall cross-link assignments.

The CID spectrum displayed in Figure 1b is strikingly different. The dominance of just a single y_6^{3+} ion fragment formed by cleavage of peptide *α* is evident. To better visualize other less intense fragment ions, the y_6^{3+} peak is plotted off scale in Figure 1c. Peptide *α* is identified based on y_2 and y_4 to y_7 ions along with a_2, b_2 to b_4, and b_7 ions; the sequence of peptide *β* is determined by y_4 to y_6, b_2, and b_3 ions. Almost all of the fragments associated with peptide *β* are extremely low in abundance, on the order of 1% of the base peak. If the experiment were conducted on a less sensitive instrument or performed with more complex protein samples, these fragments might not be detected at all. The inequivalent fragmentation of two constituent peptides, as displayed in this spectrum, is a common phenomenon when cross-links are collisionally dissociated and often leads to ambiguous identifications [15]. It is noteworthy that the P^{β}, $P^{\alpha} + L$, and $P^{\beta} + L$ peptide ions are generated from peptide/linker cleavages. This observation is consistent with our previous study with singly charged DEST cross-linked peptides showing that the amidino bonds between the linker and peptides are somewhat labile [66].

Figure 2a presents an example of a lower charged cross-link, the ETD MS^2 spectrum of the triply charged cytochrome c cross-link KATNE—GKK. Peptide *α* is confidently identified by successive c_1 to c_4 ions in addition to $a + 1_4$ ions. Neutral losses of CO_2 (43.9898 Da) and CH_3CONH_2 (59.0371 Da) from charge reduced precursors are associated with side chain cleavages of glutamic acid and asparagine respectively. Peptide *β* is matched to GKK based on c_2, $z^{\bullet}_2$, $z + 1_2$, and $a + 1_2$ ions. Since peptide *β* is so short, the protein from which it derived would be difficult to establish in most cross-linking experiments; however, this sample contains only cytochrome c. Mass pairs of P^{α}-NH_2^{1+}/$P^{\alpha} + L + NH_3^{1+}$ and P^{β}-NH_2^{1+}/$P^{\beta} + L + NH_3^{1+}$ are all observed as intense peaks, demonstrating that in the 3+ charge state cleavages at amidino groups are still favored. Note that the c_{N-1} ions of both peptides (c_4^{2+} of peptide *α* and c_2^{2+} of peptide *β*) are highly abundant. This is consistent with observations of Wysocki and coworkers that c_{N-1} ions are favored in ETD when peptides are in lower charge states (2+ and 3+) regardless of the composition of the C-terminal residues [67].

The CID MS^2 spectrum of the same cross-link, shown in Figure 2b, displays intense b_4^{2+} peptide backbone fragments. The y_1, y_2, a_1-NH_3, b_2, b_3, and b_4 ions match peptide *α*, KATNE. One side chain loss of $HCONH_2$ (45.0215 Da) from asparagine of the precursor is observed. Peptide *β* yields only cleavages between the last two residues that result in y_1, b_2-NH_3, and $b_2 + H_2O$ ions so its identification as GKK is less confident.

As an example of the ETD-induced preferential cleavage of a highly charged ion, Figure 3a displays a 6+, 573.6473 *m/z* cross-link from cytochrome c. Peptide *α* is identified as GITWKEETLMEYLENPKK based on $z^{\bullet}_1$, $z^{\bullet}_2$, $z^{\bullet}_4$ to $z^{\bullet}_{14}$, $z^{\bullet}_{16}$, y_1, y_7 to y_{11}, y_{11}, c_3 to c_7, c_9 to c_{13}, c_{17}, and $c + 1^{\bullet}_{14}$ as well as $a + 1_4$, $a + 1_7$, and $a + 1_{11}$ ions. Fragment ions c_2 to c_8, $z^{\bullet}_1$, $z^{\bullet}_3$, $z^{\bullet}_4$, $z^{\bullet}_8$, $z + 1_2$ to $z + 1_5$, $z + 1_7$, and y_1 together cover the entire sequence of peptide *β*, EDLIAYLKK. Note that fragments of peptides *α* and *β* have comparable intensities. Four intense peaks are assignable to mass pairs of P^{α}-NH_2^{2+}/$P^{\alpha} + L + NH_3^{3+}$ and P^{β}-NH_2^{1+}/$P^{\beta} + L + NH_3^{2+}$. This example demonstrates that ETD cleaves a large DEST cross-link in a high-charge state to form mass pairs related to its constituent

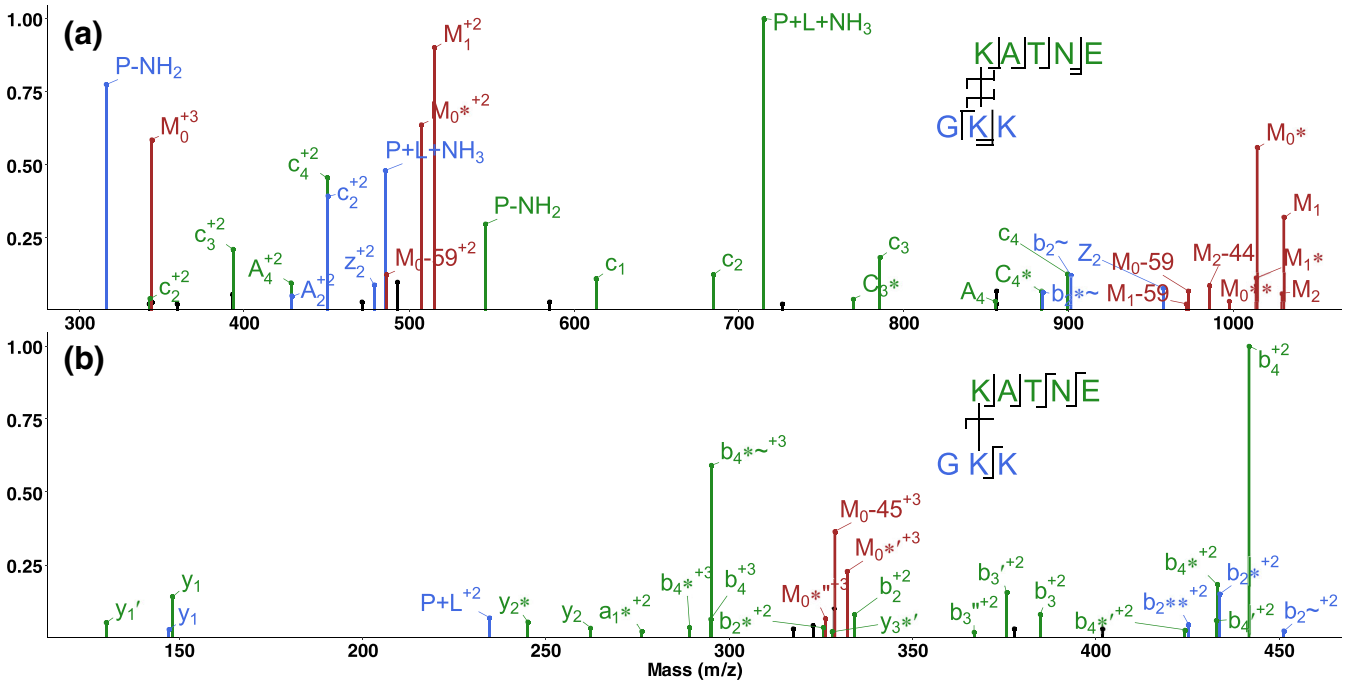

Figure 2. MS^2 spectra of the cytochrome c cross-link KATNE–GKK^{3+} at 343.8729 *m/z* fragmented by **(a)** ETD and **(b)** CID

peptides. Along with these four intense peaks, several similar peaks in different charge states are also assignable. The appearance of multiple mass pairs provides additional confidence in peptide mass assignments.

The CID spectrum of this crosslink, displayed in Figure 3b, shows that collisional activation predominantly dissociates the backbone of peptide α. Based on y_3 to y_{11}, y_{16}, b_7 to b_{12}, a_9, and a_{10} ions, many of which also lose ammonia and/or water, peptide α is identified. In contrast, peptide β yields less abundant fragments a_4-H_2O, b_4-H_2O, and b_5-H_2O. ETD yields a more confident identification of this peptide than CID.

Note that typical of ETD, precursor ions are not fragmented completely. However, more highly charged cross-links produced by DEST display higher dissociation efficiencies and more abundant peptide mass pairs and backbone fragments. An example demonstrating this is depicted in Figure S2 of Supporting Information. In this case, when the DEST crosslink TLSDYNIQKESTLHLVLR—LIFAGKQLEDGR from

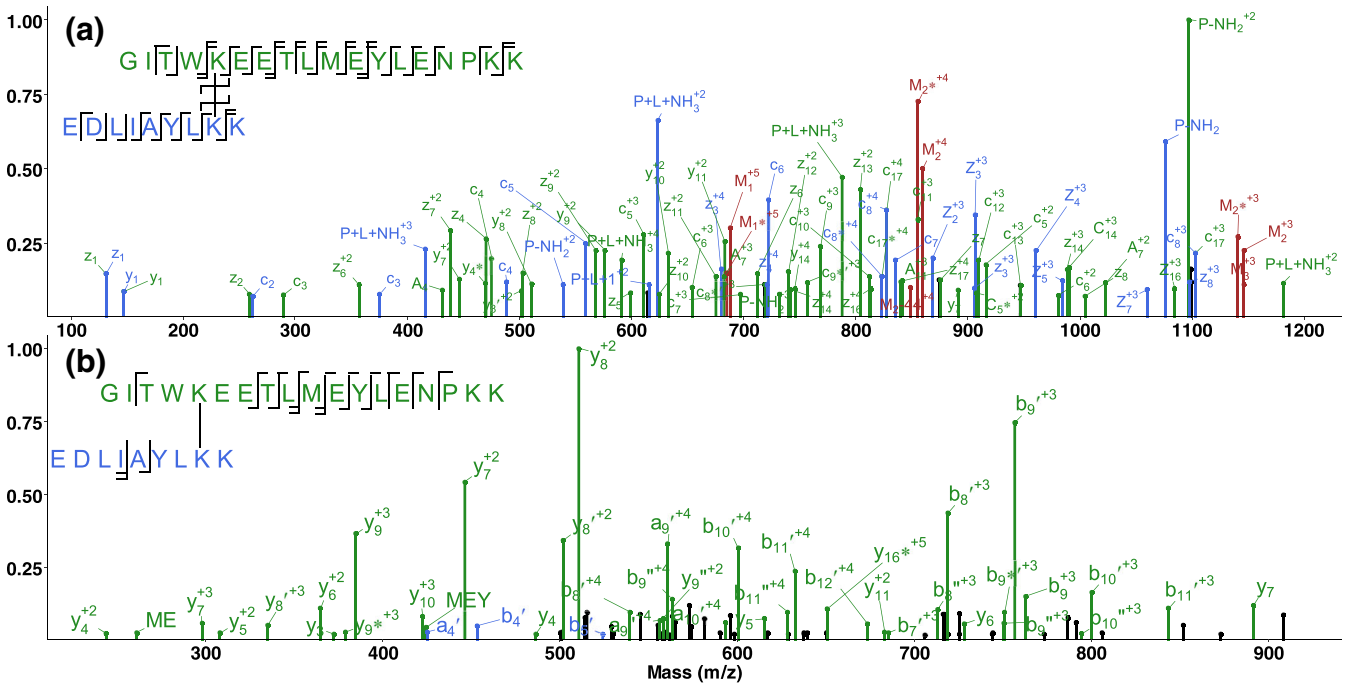

Figure 3. MS^2 spectra of the cytochrome c cross-link GITWKEETLMEYLENPKK–EDLIAYLKK^{6+} fragmented by **(a)** ETD and **(b)** CID

ubiquitin is in the 5+ charge state, precursor and charge reduced precursors are predominant though mass pairs are still among the next most intense peaks. As the charge state of this cross-link increases to 6+ and then 7+, the precursors' associated peaks become less intense while mass pairs and backbone fragments become more abundant.

Sequencing Individual Peptides of a Cross-link by MS³ Experiments

In many cases, cross-links of DEST can be identified through their ETD MS^2 spectra using mass pairs to define the masses of peptides α and β and backbone fragments to determine their sequences. However, ambiguous identifications containing isobaric or near-isobaric peptides can still arise when inadequate peptide backbone fragments appear in the ETD MS^2 spectrum or when searching a large proteome database. Further activation of ETD product ions would help to clarify ambiguous identifications or validate tentative identifications. Relatively abundant $P\text{-}NH_2$ and $P + L + NH_3$ mass pair ions are ideal precursors for MS^3 experiments. For example, a quadruply charged cross-link precursor ion at 418.7495 *m/z* from cytochrome c was activated by ETD and the resulting spectrum is displayed in Figure 4a. The most intense four peaks match two sets of mass pairs and establish the masses of peptides α and β. Peptide α is identified as acetyl-GDVEKGK based on $z^{\bullet}_1$ to $z^{\bullet}_4$, $z^{\bullet}_6$, $z + 1_3$ to $z + 1_6$, y_1, c_3 to c_6, $c + 1_6$, $a + 1_5$, and $a + 1_6$

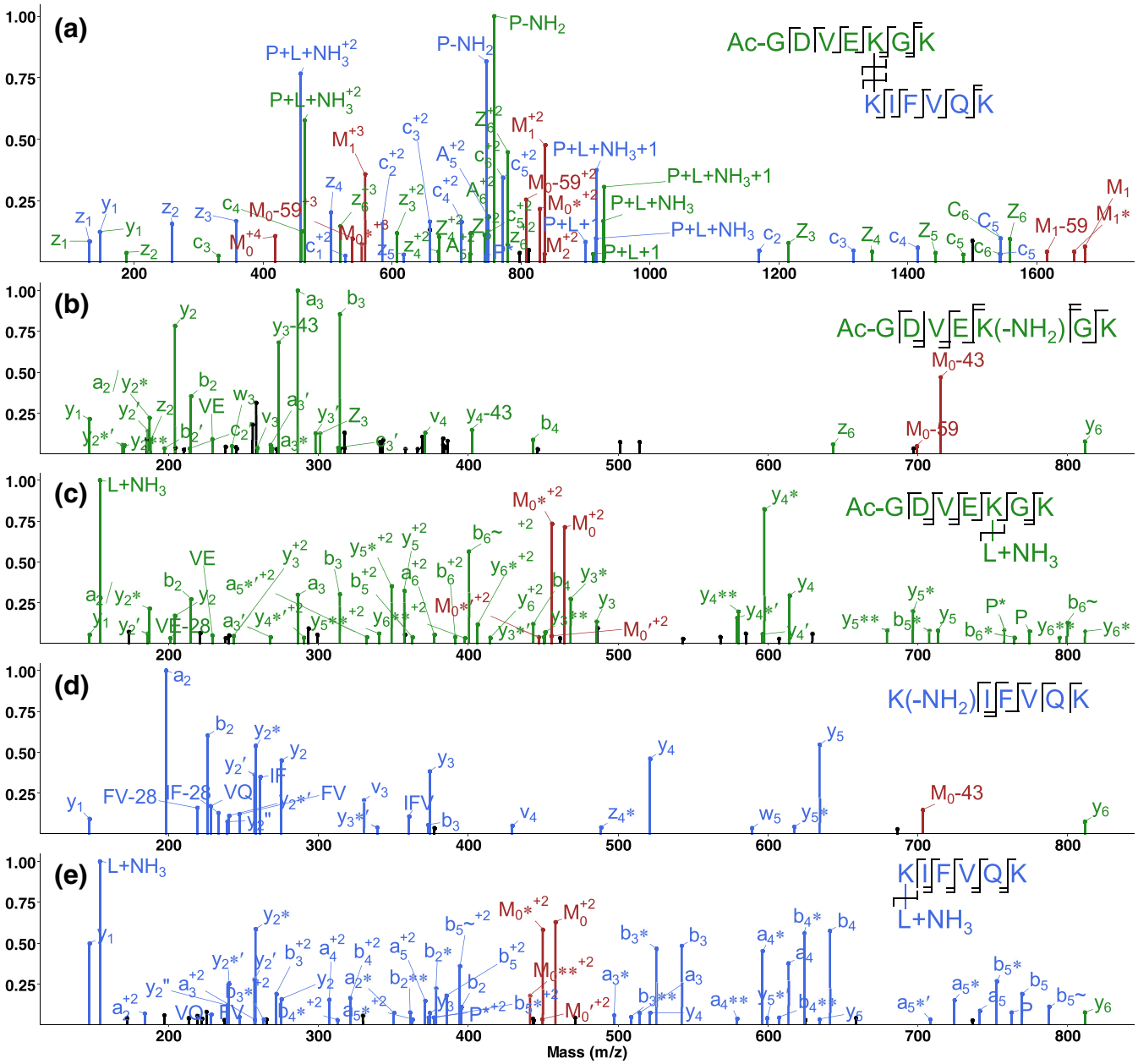

Figure 4. **(a)** ETD MS^2 spectrum of cross-link acetyl-GDVEKGK–KIFVQK^{4+} from cytochrome c. HCD MS^3 spectra derived from ETD product ions **(b)** $P^{\alpha}\text{-}NH_2{}^{1+}$, **(c)** $P^{\alpha} + L + NH_3{}^{2+}$, **(d)** $P^{\beta}\text{-}NH_2{}^{1+}$, and **(e)** $P^{\beta} + L + NH_3{}^{2+}$

ions; peptide β is assigned to KIFVQK from $z^{\bullet}_1$ to $z^{\bullet}_5$, y_1, c_1 to c_5, $c+1_5$, and $a+1_5$ ions. These assignments were next confirmed with MS^3 experiments. P-NH_2 and $P+L+NH_3$ ions were automatically selected for collisional activation by the instrument based on their mass spacing of 169.1453 Da.

The HCD MS^3 spectrum of P^{α}-NH_2 in Figure 4b yielded backbone fragments of y_1, y_2, $z^{\bullet}_2$, $z+1_3$, $z^{\bullet}_6$, a_2, b_2, b_3, and b_4, that definitively validate the sequence of acetyl-GDVEK(-NH_2)GK. The peak at 715 Da involves a neutral loss of C_3H_7 (43.1 Da or 43.055 Da measured by the orbitrap) from the precursor ion. This corresponds to a partial loss of the side chain from cross-linked lysine that had previously lost $NH_2^{\bullet}$ in the ETD process and is consistent with side chain fragmentation of activated $z^{\bullet}$-ions [68]. Since these lysine residues are prone to further loss from their side chain, analogous backbone fragments such as y_3-43 and y_4-43 also appear. Significantly, products of radical-driven fragmentation processes, such as $z^{\bullet}_2$, $z+1_3$, $z^{\bullet}_6$, v_3, and v_4, are also observed in this spectrum, consistent with P-$NH_2^{\bullet}$ being a radical ion [68].

The doubly charged partner of P^{α}-$NH_2^{\bullet}$, $P^{\alpha}+L+NH_3{}^{2+}$, was also collisionally activated and yielded the spectrum shown in Figure 4c. A full series of y-type ions from y_1 to y_6 along with b_2 to b_6, a_2, a_3, and a_6 ions validate the sequence of peptide α. The appearance of a-, b-, y-, and ammonia-loss ions is compliant with previous observations following collisional activation of c ions [68]. The base peak at 154.1 Da corresponds to L+ NH_3 that is generated by cleavage between the amidino group and the peptide. Note that this spectrum does not contain radical-derived fragments, consistent with the $P^{\alpha}+L+NH_3$ ion being an even-electron species.

Figure 4d, the HCD MS^3 spectrum of P^{β}-$NH_2^{\bullet}$, contains a full series of y ions from y_1 to y_5, a strong a_2, along with b_2, b_3, and several internal ions, such as IF, FV, and VQ. These peaks confirm the composition of peptide β. Fragments generated through radical-driven processes, such as v_3, v_4, and w_5 ions are also observed. Similar to P^{α}-$NH_2^{\bullet}$ ion, this P^{β}-$NH_2^{\bullet}$ ion also produces the unique neutral loss of 43.1 Da from the precursor, observed as a peak at 703 *m/z*.

Figure 4e shows the HCD MS^3 spectrum of $P^{\beta}+L+NH_3{}^{2+}$. Consecutive y_1 to y_5, a_2 to a_5, and b_2 to b_5 ions confirm the sequence of peptide β. The base peak at 154.1 *m/z* again corresponds to $L+NH_3$. As expected, no radical ions are detected.

The four MS^3 spectra together demonstrate that the product ions obtained by fragmentating P-$NH_2^{\bullet}$ and $P+L+NH_3$ ions provide sufficient information to validate the compositions of the two peptides. P-$NH_2^{\bullet}$ ions dissociate in different ways from their even-electron $P+L+NH_3$ counterparts, and combination of the two spectra should improve peptide and cross-link identifications [69–72].

Electron Transfer Dissociation of DEST Dead-end Peptides

Dead ends are by-products of cross-linking reactions that form when one end of the cross-linker reacts with a protein and the other end reacts with small molecules from the solution, such as water or a buffer component. Dead ends not only augment the search space but also complicate identifications when cross-links are isobaric with dead ends. Diagnostic ions that could distinguish dead ends from cross-links would improve the confidence of cross-link identifications. An ETD MS^2 spectrum of a DEST dead end from ubiquitin is displayed in Figure 5. The triply charged precursor ion at 500.9559 *m/z* is confidently identified as LIFAGKQLEDGR with a 154.1106 Da hydrolyzed dead end. Numerous $z^{\bullet}$-ions along with $z+1_8$ to $z+1_{11}$, consecutive c_5 to c_{11}, y_6 to y_8, y_{10}, as well as $a+1_6$ ion support this identification. The intense singly charged ion at 172.1444 *m/z* corresponds to hydrolyzed linker+NH_3 ($C_8N_3OH_{18}$) and serves as a dead-end reporter ion. Its complementary ion, the singly charged peptide-$NH_2^{\bullet}$ is also abundant. Its formation mechanism, analogous to that in Scheme 2, is depicted in Figure S3. In addition, reaction of one end of DEST with a peptide and the other end with free ammonium generates a dead end that adds 153.1266 Da ($C_8N_3H_{15}$) to the peptide. This type of dead end yields an abundant ion at 171.1604 *m/z* ($C_8N_4H_{19}$) (Figure S4) through the same mechanism as shown in Figure S3.

The unique masses and high abundance of 172.1444 and 171.1604 *m/z* peaks make them ideal reporter ions for dead ends. The distinctive features of reporter ions for dead ends and mass pairs for cross-links offer a simple but reliable means to differentiate dead ends from cross-links. When the labile sites of cleavable cross-links are incorporated along the spacer arm, as with most reported cleavable cross-linkers, dead ends and cross-links are endowed with identical labile sites.

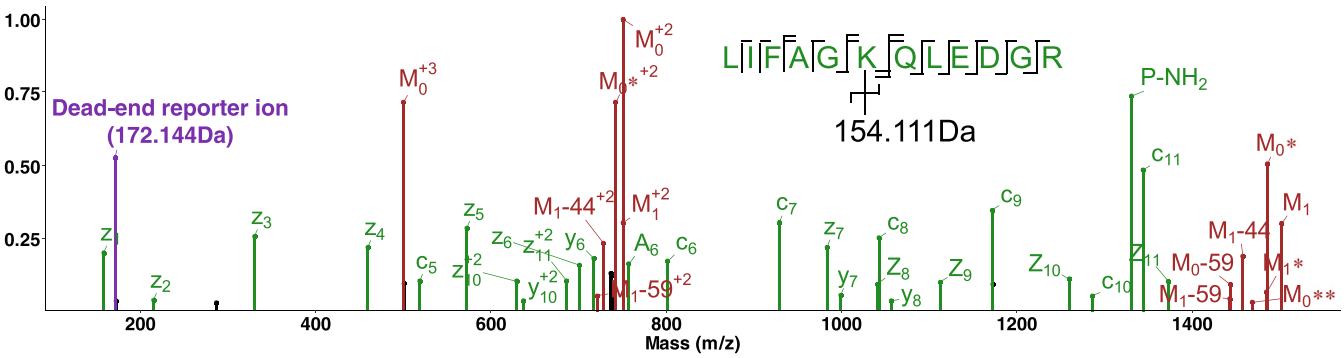

Figure 5. ETD MS^2 spectrum of the DEST hydrolyzed dead-end LIFAGK (+ 154.1106 Da) $QLEDGR^{3+}$ from ubiquitin

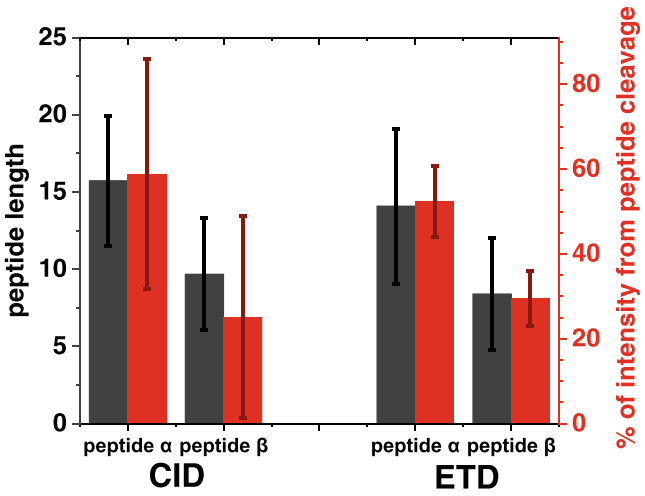

Figure 6. Comparison between peptide length (black bars) and the percentage of total fragment intensity associated with cleavage of each peptide (red bars) for CID and ETD experiments using the DEST cross-linker. Standard deviations are indicated by error bars

Consequently, dead ends and cross-links preferentially cleave at the same sites and often produce mass pairs with identical spacings. Since MS^3 peak selection is often based on predefined mass differences [73], MS^3 experiments can be triggered by dead ends. In contrast, the DEST spacer arm remains intact during ETD activation so dead ends and cross-links display different ion products. This feature should significantly reduce the chance of dead ends being fragmented in MS^3 experiments.

Comparison of Backbone Cleavage Induced by CID and ETD

An important distinguishing characteristic of ETD spectra of DEST cross-links is that they contain numerous backbone cleavages in addition to the amidino cleavages of the DEST-peptide linkages. In contrast with some CID cleavable cross-linkers, these backbone cleavages enable at least tentative identification of peptides in the MS^2 experiments. It is interesting to compare the relative proclivities of CID and ETD for inducing backbone cleavages in DEST cross-links. To do this, we considered all confidently identified cross-links from cytochrome c and ubiquitin tabulated in Tables S1 and S2 of Supporting Information except for those with constituent peptides of equal length. The average lengths of longer peptide α and shorter peptide β are represented as black bars in Figure 6. It is evident that the lengths of peptides α and β are very similar in both sets of data. The red bars display the percentage of fragment ion intensity that is associated with cleavage of the two peptides in the two experiments. Intensities of characteristic ions, such as P and P + L yielded by CID as well as P-$NH_2^{\bullet}$ and P + L + NH_3 formed with ETD are counted towards their corresponding peptides. It is clear that the relative fragmentation of peptides α and β by ETD is simply proportional to their lengths indicating that the average likelihood of a backbone bond being fragmented by ETD is similar in both longer and shorter peptides. In contrast, CID cleaves peptide β less efficiently than peptide α. This is probably because longer peptides have larger collision cross sections and the energy gained during activation may not be effectively transferred to the smaller peptide. The distribution of fragment intensities assigned to peptides α and β also appears to be wider in CID than with ETD as indicated by error bars representing one standard deviation. It is noteworthy that CID backbone cleavage propensities can be quite sequence dependent [74–76] and this can make it harder to identify peptides of cross-links. This is exemplified in Figure 1b, where the CID favored cleavage between I and F leads to a_2, b_2, and y_6^{3+} ions, the latter being particularly intense, but most other backbone fragments are much lower in abundance. Since positive charges repel each other, the protons on a DEST cross-link are likely to be distributed over both peptides. Therefore, it is not surprising to see comparable backbone fragmentation induced by ETD. This characteristic should improve the confidence of identifying both peptides involved in a cross-link, which is why cross-links of DEST can often be confidently identified based on just ETD MS^2 spectra. The above statistical analysis was conducted using cytochrome c and ubiquitin cross-links, and it could be improved with a larger study. In comparison to prevalent workflows with other cleavable cross-linkers that often require the combination of one MS^2 spectrum with multiple MS^3

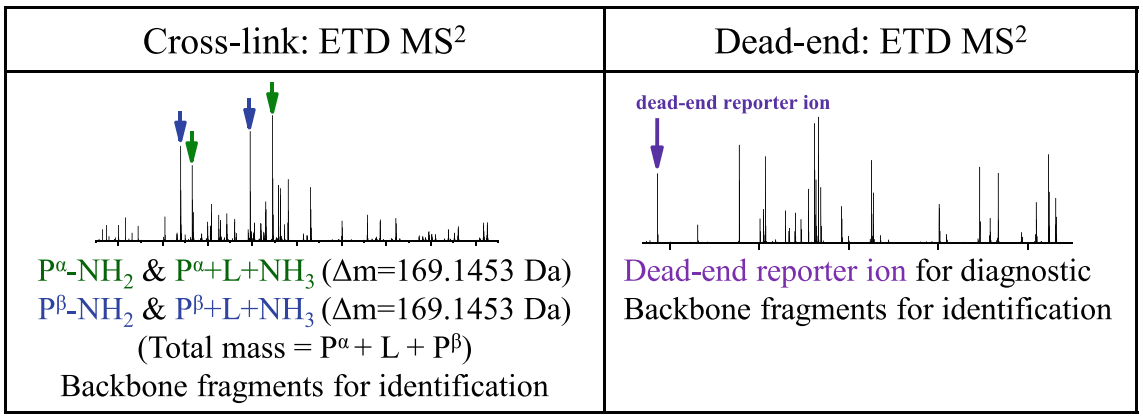

Scheme 3. Unique ETD fragment patterns of DEST cross-links and dead ends

spectra to identify a cross-link, ETD fragmentation of DEST cross-links yields both mass pairs and backbone cleavages that enable their identification.

Key Attributes of ETD Strategy with DEST Cross-links

The results presented above demonstrate that when fragmented with ETD, DEST cross-links yield peptide mass pairs along with backbone fragments while dead ends form reporter ions. This allows us to propose a strategy for arriving at confident cross-linked peptide identifications. As depicted in Scheme 3, precursors are initially fragmented by ETD. In the resulting MS^2 spectra, cross-links are diagnosed by mass pairs and identified through additional peptide backbone fragments. Dead ends are discernable from cross-links on-the-fly due to their unique reporter ions and the absence of mass pairs. Detection of a dead-end reporter ion along with the absence of two sets of mass pairs provides a simple yet effective means to discriminate dead ends from cross-links. To validate MS^2 identifications of cross-links, ETD mass pairs, product ions with mass spacings of 169.1453 Da, are fragmented in MS^3 experiments. Dissociation of either the P-$NH_2^{\bullet}$ or the P + L + NH_3 ion of a mass pair may be sufficient, although having the complementary data from both ions is generally advantageous.

Applications of the DEST Cross-linking Strategy to Model Proteins

Previously, SCX enrichment and fractionation have proven to be effective tools to identify more DEST cross-links in complex samples. The two positive charges retained on the amidine groups certainly facilitate this process [12]. Due to the simplicity of the samples in this study, SCX enrichment was not employed. All cross-links of cytochrome c and ubiquitin confidently identified are listed in Tables S1 and S2 respectively. Comparisons of unique cross-linking pairs identified by ETD and CID approaches are displayed in Tables S3 and S4. The numbers of unique DEST cross-links observed in cytochrome c and ubiquitin are comparable to those that have been reported in previous studies with DSSO [25] and DUCCT [41]. A few of the cross-linking sites are different (Table S5), possibly due to differences in cross-linker polarities. The distances between C_α of each linked residue pair were calculated based on their crystal structures, and all are less than 24 Å, as expected for cross-linkers of this length.

Conclusions

We have demonstrated a novel ETD-induced cleavage mechanism associated with amidine groups that efficiently cleaves DEST cross-links. Cross-links of DEST preferentially dissociate at the amidine groups yielding mass pairs P-$NH_2^{\bullet}$/P + L + NH_3 of both constituent peptides. Simultaneously, backbones of the two peptides cleave. As a result, DEST cross-links can often be identified from single ETD MS^2 spectra. Additionally, dead ends generate strong reporter ions through the same mechanism. The substantially different diagnostic characteristics of cross-links and dead ends enable them to be distinguished. On-the-fly MS^3 experiments on peptide mass pairs can be used to validate sequences tentatively identified in MS^2 spectra. P-$NH_2^{\bullet}$ radical ions and their even-electron P + L + NH_3 counterparts dissociate to yield somewhat different products. This DEST cross-linking workflow provides a simple but reliable approach to confidently identify cross-links and potentially enable high-throughput experiments with protein complexes or networks.

Acknowledgements

We would like to thank Dr. Jonathan Meek for the spectrum plotting program. This work was supported by the National Institutes of Health grants R01 GM103725 and U54 GM074807. It was partially funded by the Indiana University Vice Provost for Research through the Faculty Research Support Program.

References

1. Young, M.M., Tang, N., Hempel, J.C., Oshiro, C.M., Taylor, E.W., Kuntz, I.D., Gibson, B.W., Dollinger, G.: High throughput protein fold identification by using experimental constraints derived from intramolecular cross-links and mass spectrometry. Proc. Natl. Acad. Sci. U. S. A. **97**, 5802–5806 (2000)
2. Sinz, A.: Chemical cross-linking and mass spectrometry to map three-dimensional protein structures and protein-protein interactions. Mass Spectrom. Rev. **25**, 663–682 (2006)
3. Leitner, A., Walzthoeni, T., Kahraman, A., Herzog, F., Rinner, O., Beck, M., Aebersold, R.: Probing native protein structures by chemical cross-linking, mass spectrometry, and bioinformatics. Mol. Cell. Proteomics. **9**, 1634–1649 (2010)
4. Merkley, E.D., Cort, J.R., Adkins, J.N.: Cross-linking and mass spectrometry methodologies to facilitate structural biology: finding a path through the maze. J. Struct. Funct. Genom. **14**, 77–90 (2013)
5. Yu, C., Huang, L.: Cross-linking mass spectrometry: an emerging technology for interactomics and structural biology. Anal. Chem. **90**, 144–165 (2018)
6. Kim, S.J., Fernandez-Martinez, J., Nudelman, I., Shi, Y., Zhang, W., Raveh, B., Herricks, T., Slaughter, B.D., Hogan, J.A., Upla, P., Chemmama, I.E., Pellarin, R., Echeverria, I., Shivaraju, M., Chaudhury, A.S., Wang, J., Williams, R., Unruh, J.R., Greenberg, C.H., Jacobs, E.Y., Yu, Z., de la Cruz, M.J., Mironska, R., Stokes, D.L., Aitchison, J.D., Jarrold, M.F., Gerton, J.L., Ludtke, S.J., Akey, C.W., Chait, B.T., Sali, A., Rout, M.P.: Integrative structure and functional anatomy of a nuclear pore complex. Nature. **555**, 475–482 (2018)
7. Wang, X., Cimermancic, P., Yu, C., Schweitzer, A., Chopra, N., Engel, J.L., Greenberg, C., Huszagh, A.S., Beck, F., Sakata, E., Yang, Y., Novitsky, E.J., Leitner, A., Nanni, P., Kahraman, A., Guo, X., Dixon, J.E., Rychnovsky, S.D., Aebersold, R., Baumeister, W., Sali, A., Huang, L.: Molecular details underlying dynamic structures and regulation of the human 26S proteasome. Mol. Cell. Proteomics. **16**, 840–854 (2017)
8. Robinson, P.J., Trnka, M.J., Bushnell, D.A., Davis, R.E., Mattei, P.J., Burlingame, A.L., Kornberg, R.D.: Structure of a complete mediator-RNA polymerase II pre-initiation complex. Cell. **166**, 1411–1422 e1416 (2016)
9. Arlt, C., Ihling, C.H., Sinz, A.: Structure of full-length p53 tumor suppressor probed by chemical cross-linking and mass spectrometry. Proteomics. **15**, 2746–2755 (2015)
10. Zeng-Elmore, X., Gao, X.Z., Pellarin, R., Schneidman-Duhovny, D., Zhang, X.J., Kozacka, K.A., Tang, Y., Sali, A., Chalkley, R.J., Cote, R.H., Chu, F.: Molecular architecture of photoreceptor phosphodiesterase

elucidated by chemical cross-linking and integrative modeling. J. Mol. Biol. **426**, 3713–3728 (2014)
11. Lauber, M.A., Rappsilber, J., Reilly, J.P.: Dynamics of ribosomal protein S1 on a bacterial ribosome with cross-linking and mass spectrometry. Mol. Cell. Proteomics. **11**, 1965–1976 (2012)
12. Lauber, M.A., Reilly, J.P.: Structural analysis of a prokaryotic ribosome using a novel amidinating cross-linker and mass spectrometry. J. Proteome Res. **10**, 3604–3616 (2011)
13. Schweppe, D.K., Chavez, J.D., Lee, C.F., Caudal, A., Kruse, S.E., Stuppard, R., Marcinek, D.J., Shadel, G.S., Tian, R., Bruce, J.E.: Mitochondrial protein interactome elucidated by chemical cross-linking mass spectrometry. Proc. Natl. Acad. Sci. U. S. A. **114**, 1732–1737 (2017)
14. Liu, F., Rijkers, D.T., Post, H., Heck, A.J.: Proteome-wide profiling of protein assemblies by cross-linking mass spectrometry. Nat. Methods. **12**, 1179–1184 (2015)
15. Trnka, M.J., Baker, P.R., Robinson, P.J., Burlingame, A.L., Chalkley, R.J.: Matching cross-linked peptide spectra: only as good as the worse identification. Mol. Cell. Proteomics. **13**, 420–434 (2014)
16. Iacobucci, C., Sinz, A.: To be or not to be? Five guidelines to avoid misassignments in cross-linking/mass spectrometry. Anal. Chem. **89**, 7832–7835 (2017)
17. Sinz, A.: Divide and conquer: cleavable cross-linkers to study protein conformation and protein-protein interactions. Anal. Bioanal. Chem. **409**, 33–44 (2017)
18. Tang, X., Munske, G.R., Siems, W.F., Bruce, J.E.: Mass spectrometry identifiable cross-linking strategy for studying protein-protein interactions. Anal. Chem. **77**, 311–318 (2005)
19. Chowdhury, S.M., Munske, G.R., Tang, X., Bruce, J.E.: Collisionally activated dissociation and electron capture dissociation of several mass spectrometry-identifiable chemical cross-linkers. Anal. Chem. **78**, 8183–8193 (2006)
20. Soderblom, E.J., Goshe, M.B.: Collision-induced dissociative chemical cross-linking reagents and methodology: applications to protein structural characterization using tandem mass spectrometry analysis. Anal. Chem. **78**, 8059–8068 (2006)
21. Soderblom, E.J., Bobay, B.G., Cavanagh, J., Goshe, M.B.: Tandem mass spectrometry acquisition approaches to enhance identification of protein-protein interactions using low-energy collision-induced dissociative chemical crosslinking reagents. Rapid Commun. Mass Spectrom. **21**, 3395–3408 (2007)
22. Liu, F., Goshe, M.B.: Combinatorial electrostatic collision-induced dissociative chemical cross-linking reagents for probing protein surface topology. Anal. Chem. **82**, 6215–6223 (2010)
23. Muller, M.Q., Dreiocker, F., Ihling, C.H., Schafer, M., Sinz, A.: Cleavable cross-linker for protein structure analysis: reliable identification of cross-linking products by tandem MS. Anal. Chem. **82**, 6958–6968 (2010)
24. Hage, C., Falvo, F., Schafer, M., Sinz, A.: Novel concepts of MS-cleavable cross-linkers for improved peptide structure analysis. J. Am. Soc. Mass Spectrom. **28**, 2022–2038 (2017)
25. Kao, A., Chiu, C.L., Vellucci, D., Yang, Y., Patel, V.R., Guan, S., Randall, A., Baldi, P., Rychnovsky, S.D., Huang, L.: Development of a novel cross-linking strategy for fast and accurate identification of cross-linked peptides of protein complexes. Mol. Cell. Proteomics. **10**, M110 002212 (2011)
26. Kaake, R.M., Wang, X., Burke, A., Yu, C., Kandur, W., Yang, Y., Novtisky, E.J., Second, T., Duan, J., Kao, A., Guan, S., Vellucci, D., Rychnovsky, S.D., Huang, L.: A new in vivo cross-linking mass spectrometry platform to define protein-protein interactions in living cells. Mol. Cell. Proteomics. **13**, 3533–3543 (2014)
27. Yu, C., Kandur, W., Kao, A., Rychnovsky, S., Huang, L.: Developing new isotope-coded mass spectrometry-cleavable cross-linkers for elucidating protein structures. Anal. Chem. **86**, 2099–2106 (2014)
28. Clifford-Nunn, B., Showalter, H.D., Andrews, P.C.: Quaternary diamines as mass spectrometry cleavable crosslinkers for protein interactions. J. Am. Soc. Mass Spectrom. **23**, 201–212 (2012)
29. Petrotchenko, E.V., Serpa, J.J., Borchers, C.H.: An isotopically coded CID-cleavable biotinylated cross-linker for structural proteomics. Mol. Cell. Proteomics. **10**, M110 001420 (2011)
30. Gotze, M., Pettelkau, J., Fritzsche, R., Ihling, C.H., Schafer, M., Sinz, A.: Automated assignment of MS/MS cleavable cross-links in protein 3D-structure analysis. J. Am. Soc. Mass Spectrom. **26**, 83–97 (2015)
31. Syka, J.E., Coon, J.J., Schroeder, M.J., Shabanowitz, J., Hunt, D.F.: Peptide and protein sequence analysis by electron transfer dissociation mass spectrometry. Proc. Natl. Acad. Sci. U. S. A. **101**, 9528–9533 (2004)
32. Catherman, A.D., Durbin, K.R., Ahlf, D.R., Early, B.P., Fellers, R.T., Tran, J.C., Thomas, P.M., Kelleher, N.L.: Large-scale top-down proteomics of the human proteome: membrane proteins, mitochondria, and senescence. Mol. Cell. Proteomics. **12**, 3465–3473 (2013)
33. Toby, T.K., Fornelli, L., Kelleher, N.L.: Progress in top-down proteomics and the analysis of Proteoforms. Annu. Rev. Anal. Chem. **9**, 499–519 (2016)
34. Riley, N.M., Coon, J.J.: The role of electron transfer dissociation in modern proteomics. Anal. Chem. **90**, 40–64 (2018)
35. Chi, A., Huttenhower, C., Geer, L.Y., Coon, J.J., Syka, J.E.P., Bai, D.L., Shabanowitz, J., Burke, D.J., Troyanskaya, O.G., Hunt, D.F.: Analysis of phosphorylation sites on proteins from Saccharomyces cerevisiae by electron transfer dissociation (ETD) mass spectrometry. Proc. Natl. Acad. Sci. U. S. A. **104**, 2193–2198 (2007)
36. Desaire, H.: Glycopeptide analysis, recent developments and applications. Mol. Cell. Proteomics. **12**, 893–901 (2013)
37. Good, D.M., Wirtala, M., McAlister, G.C., Coon, J.J.: Performance characteristics of electron transfer dissociation mass spectrometry. Mol. Cell. Proteomics. **6**, 1942–1951 (2007)
38. Frese, C.K., Altelaar, A.F.M., Hennrich, M.L., Nolting, D., Zeller, M., Griep-Raming, J., Heck, A.J.R., Mohammed, S.: Improved peptide identification by targeted fragmentation using CID, HCD and ETD on an LTQ-Orbitrap Velos. J. Proteome Res. **10**, 2377–2388 (2011)
39. Kolbowski, L., Mendes, M.L., Rappsilber, J.: Optimizing the parameters governing the fragmentation of cross-linked peptides in a tribrid mass spectrometer. Anal. Chem. **89**, 5311–5318 (2017)
40. Gardner, M.W., Brodbelt, J.S.: Preferential cleavage of N-N hydrazone bonds for sequencing bis-arylhydrazone conjugated peptides by electron transfer dissociation. Anal. Chem. **82**, 5751–5759 (2010)
41. Chakrabarty, J.K., Naik, A.G., Fessler, M.B., Munske, G.R., Chowdhury, S.M.: Differential tandem mass spectrometry-based cross-linker: a new approach for high confidence in identifying protein cross-linking. Anal. Chem. **88**, 10215–10222 (2016)
42. Trnka, M.J., Burlingame, A.L.: Topographic studies of the GroEL-GroES chaperonin complex by chemical cross-linking using diformyl ethynylbenzene: the power of high resolution electron transfer dissociation for determination of both peptide sequences and their attachment sites. Mol. Cell. Proteomics. **9**, 2306–2317 (2010)
43. Leitner, A., Joachimiak, L.A., Unverdorben, P., Walzthoeni, T., Frydman, J., Forster, F., Aebersold, R.: Chemical cross-linking/mass spectrometry targeting acidic residues in proteins and protein complexes. Proc. Natl. Acad. Sci. U. S. A. **111**, 9455–9460 (2014)
44. Gutierrez, C.B., Yu, C., Novitsky, E.J., Huszagh, A.S., Rychnovsky, S.D., Huang, L.: Developing an acidic residue reactive and sulfoxide-containing MS-cleavable homobifunctional cross-linker for probing protein-protein interactions. Anal. Chem. **88**, 8315–8322 (2016)
45. Belsom, A., Mudd, G., Giese, S., Auer, M., Rappsilber, J.: Complementary benzophenone cross-linking/mass spectrometry photochemistry. Anal. Chem. **89**, 5319–5324 (2017)
46. Luo, J., Fishburn, J., Hahn, S., Ranish, J.: An integrated chemical cross-linking and mass spectrometry approach to study protein complex architecture and function. Mol. Cell. Proteomics. **11**, (2012)
47. Hage, C., Iacobucci, C., Rehkamp, A., Arlt, C., Sinz, A.: The first zero-length mass spectrometry-cleavable cross-linker for protein structure analysis. Angew. Chem. Int. Ed. Eng. **56**, 14551–14555 (2017)
48. Lauber, M.A., Reilly, J.P.: Novel amidinating cross-linker for facilitating analyses of protein structures and interactions. Anal. Chem. **82**, 7736–7743 (2010)
49. Chaturvedi, R.K., MacMahon, A.E., Schmir, G.L.: The hydrolysis of thioimidate esters. Tetrahedral intermediates and general acid catalysis. J. Am. Chem. Soc. **89**, 6984–6993 (1967)
50. Beardsley, R.L., Reilly, J.P.: Fragmentation of amidinated peptide ions. J. Am. Soc. Mass Spectrom. **15**, 158–167 (2004)
51. Beardsley, R.L., Reilly, J.P.: Quantitation using enhanced signal tags: a technique for comparative proteomics. J. Proteome Res. **2**, 15–21 (2003)
52. Sharon, L.A., Beardsley, R.L., Reilly, J.P.: Derivatization of tryptic peptides to facilitate de novo sequencing. Abstr. Pap. Am. Chem. Soc. **227**, U609–U609 (2004)
53. Beardsley, R.L., Sharon, L.A., Reilly, J.P.: Peptide de novo sequencing facilitated by a dual-labeling strategy. Anal. Chem. **77**, 6300–6309 (2005)
54. Janecki, D.J., Beardsley, R.L., Reilly, J.P.: Probing protein tertiary structure with amidination. Anal. Chem. **77**, 7274–7281 (2005)

55. Liu, X., Broshears, W.C., Reilly, J.P.: Probing the structure and activity of trypsin with amidination. Anal. Biochem. **367**, 13–19 (2007)
56. Running, W.E., Reilly, J.P.: Ribosomal proteins of Deinococcus radiodurans: their solvent accessibility and reactivity. J. Proteome Res. **8**, 1228–1246 (2009)
57. Liu, X., Reilly, J.P.: Correlating the chemical modification of Escherichia coli ribosomal proteins with crystal structure data. J. Proteome Res. **8**, 4466–4478 (2009)
58. Beardsley, R.L., Running, W.E., Reilly, J.P.: Probing the structure of the Caulobacter crescentus ribosome with chemical labeling and mass spectrometry. J. Proteome Res. **5**, 2935–2946 (2006)
59. Browne, D.T., Kent, S.B.H.: Formation of non-amidine products in reaction of primary amines with imido esters. Biochem. Biophys. Res. Commun. **67**, 126–132 (1975)
60. Dihazi, G.H., Sinz, A.: Mapping low-resolution three-dimensional protein structures using chemical cross-linking and Fourier transform ion-cyclotron resonance mass spectrometry. Rapid Commun. Mass Spectrom. **17**, 2005–2014 (2003)
61. Koolen, H.H., Gomes, A.F., Schwab, N.V., Eberlin, M.N., Gozzo, F.C.: Imidate-based cross-linkers for structural proteomics: increased charge of protein and peptide ions and CID and ECD fragmentation studies. J. Am. Soc. Mass Spectrom. **25**, 1181–1191 (2014)
62. Li, S., Dabir, A., Misal, S.A., Tang, H., Radivojac, P., Reilly, J.P.: Impact of amidination on peptide fragmentation and identification in shotgun proteomics. J. Proteome Res. **15**, 3656–3665 (2016)
63. Zubarev, R.A., Kelleher, N.L., McLafferty, F.W.: Electron capture dissociation of multiply charged protein cations. a nonergodic process. J. Am. Chem. Soc. **120**, 3265–3266 (1998)
64. Turecek, F., Syrstad, E.A.: Mechanism and energetics of intramolecular hydrogen transfer in amide and peptide radicals and cation-radicals. J. Am. Chem. Soc. **125**, 3353–3369 (2003)
65. Zhurov, K.O., Fornelli, L., Wodrich, M.D., Laskay, U.A., Tsybin, Y.O.: Principles of electron capture and transfer dissociation mass spectrometry applied to peptide and protein structure analysis. Chem. Soc. Rev. **42**, 5014–5030 (2013)
66. He, Y., Lauber, M.A., Reilly, J.P.: Unique fragmentation of singly charged DEST cross-linked peptides. J. Am. Soc. Mass Spectrom. **23**, 1046–1052 (2012)
67. Li, W., Song, C., Bailey, D.J., Tseng, G.C., Coon, J.J., Wysocki, V.H.: Statistical analysis of electron transfer dissociation pairwise fragmentation patterns. Anal. Chem. **83**, 9540–9545 (2011)
68. Han, H., Xia, Y., McLuckey, S.A.: Ion trap collisional activation of c and z* ions formed via gas-phase ion/ion electron-transfer dissociation. J. Proteome Res. **6**, 3062–3069 (2007)
69. Xia, Y., Chrisman, P.A., Pitteri, S.J., Erickson, D.E., McLuckey, S.A.: Ion/molecule reactions of cation radicals formed from protonated polypeptides via gas-phase ion/ion electron transfer. J. Am. Chem. Soc. **128**, 11792–11798 (2006)
70. Ly, T., Julian, R.R.: Residue-specific radical-directed dissociation of whole proteins in the gas phase. J. Am. Chem. Soc. **130**, 351–358 (2008)
71. Sun, Q., Nelson, H., Ly, T., Stoltz, B.M., Julian, R.R.: Side chain chemistry mediates backbone fragmentation in hydrogen deficient peptide radicals. J. Proteome Res. **8**, 958–966 (2009)
72. Iacobucci, C., Schafer, M., Sinz, A.: Free radical-initiated peptide sequencing (FRIPS)-based cross-linkers for improved peptide and protein structure analysis. Mass Spectrom. Rev. (2018)
73. Liu, F., Lossl, P., Scheltema, R., Viner, R., Heck, A.J.R.: Optimized fragmentation schemes and data analysis strategies for proteome-wide cross-link identification. Nat. Commun. **8**, 15473 (2017)
74. Breci, L.A., Tabb, D.L., Yates, J.R., Wysocki, V.H.: Cleavage N-terminal to proline: analysis of a database of peptide tandem mass spectra. Anal. Chem. **75**, 1963–1971 (2003)
75. Gu, C., Tsaprailis, G., Breci, L., Wysocki, V.H.: Selective gas-phase cleavage at the peptide bond C-terminal to aspartic acid in fixed-charge derivatives of Asp-containing peptides. Anal. Chem. **72**, 5804–5813 (2000)
76. Huang, Y., Triscari, J.M., Tseng, G.C., Pasa-Tolic, L., Lipton, M.S., Smith, R.D., Wysocki, V.H.: Statistical characterization of the charge state and residue dependence of low-energy CID peptide dissociation patterns. Anal. Chem. **77**, 5800–5813 (2005)